FOREX Publication
Open Access | Rapid and quality publishing

International Journal of
Electrical and Electronics Research (IJEER)
Review Article | Volume 13, Issue 4 | Pages 943-953 | e-ISSN: 2347-470X

Coordinated Control of Grid-Connected Solar and Wind Power for Electric Vehicle Charging and Power Quality Enhancement Using DPFC

M Suvarna[1*], M Ramasekhara Reddy[2], and K Nagabhushanam[3]
[1]M.Tech, EEE Dept., Jawaharlal Nehru Technological University, Ananthapur, Andhra Pradesh, India; Email: Sweetysuvarna17@gmail.com
[2]Associate Professor, EEE Dept., Jawaharlal Nehru Technological University, Ananthapur, Andhra Pradesh, India; Email: ramasekharreddy.eee@jntua.ac.in
[3]Assistant Professor (Adhoc), EEE Dept., Jawaharlal Nehru Technological University, Ananthapur, Andhra Pradesh, India; Email: Knneee.eee@jntua.ac.in

***Correspondence:** *M Suvarna, Email: Sweetysuvarna17@gmail.com; Tel.: +91 6302755453*

ABSTRACT- Numerous converters enhance the flexibility and manageability of the Grid-Connected Converter (GCC) within a DC/AC microgrid, facilitating the smooth incorporation of renewable energy sources. To capitalize on the power generation from photovoltaic (PV) modules and the wind turbines MPPT technique is employed. A DC voltage regulator is used in the layer of primary control to sustain a stable voltage profile. A coordinated control strategy integrates a grid-connected solar and wind power generation system with electric vehicle (EV) charging stations, balancing AC-DC loads with the support of a battery storage system. The solar PV system incorporates a boost converter with a Circle Search MPPT algorithm to optimize power extraction. The combination of wind and solar energy improves system reliability, ensuring renewable power supply for EV charging and household loads. The Power quality issues, such as the voltage sags and swells, are mitigated using a Distributed Power Flow Conditioner (DPFC), which enhances overall power quality and confirms stable procedure of the distribution system. The proposed system is tested in a MATLAB/Simulink environment, where the control strategy effectively balances loads, optimizes power delivery, and improves power quality under varying conditions.

Keywords: DC/AC microgrid, battery energy storage system, Circle search Algorithm coordinated control, photovoltaic energy, Wind energy.

ARTICLE INFORMATION
Author(s): M Suvarna, M Ramasekhara Reddy, and K Nagabhushanam;
Received: 03/09/2025; **Accepted:** 15/12/2025; **Published:** 30/12/2025;
E- ISSN: 2347-470X;
Paper Id: IJEER 250141;
Citation: 10.37391/ijeer.130434
Webpage-link:
https://ijeer.forexjournal.co.in/archive/volume-13/ijeer-130434.html

1. INTRODUCTION

Microgrid technology is anticipated to become more and more important in future power systems as it is fast-developing innovation in the power industry and of its many benefits. This idea was presented as a way to smoothly integrate several power generation sources without interfering with the utility grid, especially when renewable energy is included. Efficiency, dependability, cost-effectiveness, safe grid integration, microgrid management capabilities, energy storage options, low environmental impact, and the development of complex control and monitoring algorithms are just a few of the crucial elements that make up renewable energy sources.

Photovoltaic (PV), wind, and hydroelectric power are the most common renewable energy sources. The PV industry is growing at a pace of more than 30% per year, even if hydroelectric electricity is still the most common source. An effective maximum power point tracking (MPPT) is necessary since PV energy is intermittent and nonlinear, with power production varying depending on environmental factors. Renewable energy resource (RER) integration within the utility grid is gaining popularity due to its affordability; nonetheless, power quality problems are mostly caused by changes in RER power output.

To maximize power extraction from photovoltaic (PV) modules, several maximum power point tracking (MPPT) algorithms have been developed. The perturb and observe (P&O) approach [1], incremental conductance (Inc) [2], and the hill-climbing algorithm [3], are some of the most used. Because of its great efficiency, capacity to capture the most wind power, decreased power fluctuations, the adjustable-speed wind turbine built on a permanent magnet synchronous generator (PMSG) is frequently used in industrial claims [4]. Numerous tracking algorithms have been created to maximize the amount of power extracted from wind turbines [5],[6]. While power electronic converters have

FOREX Publication
Open Access | Rapid and quality publishing
International Journal of Electrical and Electronics Research (IJEER)
Review Article | Volume 13, Issue 4 | Pages 943-953|e-ISSN: 2347-470X

nonlinear features that result in voltage and current harmonics at the PCC connection, wind velocity and solar irradiance behave stochastically. LCL filters have drawn a lot of interest because of their superior harmonic reduction qualities, small size, and lightweight construction [7]. But their design necessitates a lot of mathematical calculations.

The Distributed Power Flow Controller (DPFC), installed at the point of common coupling (PCC), is identified as an effective custom power device for mitigating voltage- and current-related power quality (PQ) issues in distribution systems [13],[14]. Its primary function is to enhance PQ through voltage regulation and mitigation of disturbances such as sags, swells, and harmonics. The DPFC comprises a shunt active power filter (ShAPF) and a series active power filter (SeAPF) linked by a common DC bus. While the ShAPF suppresses current-related issues [15], including harmonics and reactive power demand, and maintains DC-link voltage, the SeAPF addresses voltage disturbances such as sags and swells [16].

The integration of renewable energy sources (RES) into power networks is a major research focus due to their potential to enhance system performance [21],[22]. Solar photovoltaic (PV) systems, in particular, contribute to sustainability and carbon emission reduction. Their integration with the Unified Power Quality Conditioner (UPQC) can provide additional technical and environmental benefits.

For effective operation of the Unified Power Quality Conditioner (UPQC), an appropriate control strategy must generate the reference load voltage signal and the source current signal to drive the series and shunt compensators, respectively. Several studies have employed conventional time-domain control techniques, including Instantaneous Symmetrical Component Theory (ISCT), Synchronous Reference Frame (SRF or d–q–0), and Instantaneous Reactive Power Theory (IRPT or p–q) [23].

The key contributions of this paper include optimize power extraction from the wind and PV panels; a circle search algorithm and tip-speed ratio technique are applied. In order to maintain a steady DC bus voltage during grid outages, an embedded energy storage device with a bidirectional DC-DC converter is connected to the shared DC bus and is affected by changes in solar radiation and wind speed. The implementation of inductor current reference generation and a generalized power flow management system maximize the utilization of renewable energy sources while reducing dependence on grid power. To transfer surplus energy to the utility grid and provide a dependable power supply to local loads, A cooperative control system with two layers is implemented.

2. OUTLINE OF DC/AC MICROGRID

Figure 1 displays the inclusive block diagram for the DC/AC microgrid system. The system comprises a wind energy conversion system that utilizes a permanent magnet synchronous motor (PMSM), a bidirectional converter integrated within an energy storage device, an active rectifier, a photovoltaic (PV) panel equipped with a boost converter, a water pump controlled by a variable frequency drive, a DC link capacitor, a grid-connected converter, an LCL filter, a DC load, a relay that activates during islanded operation, and a power supply.

In this system, the active 3-Φ rectifier is controlled to maximize wind power, while the boost converter is regulated to maximize PV output. The battery-connected bidirectional converter keeps the DC bus voltage steady. Interaction with the utility grid is facilitated by the grid-connected converter, where the real power from renewable energy sources and the power castoff by the limited load are used to generate the reference inductor current for the inner loop.

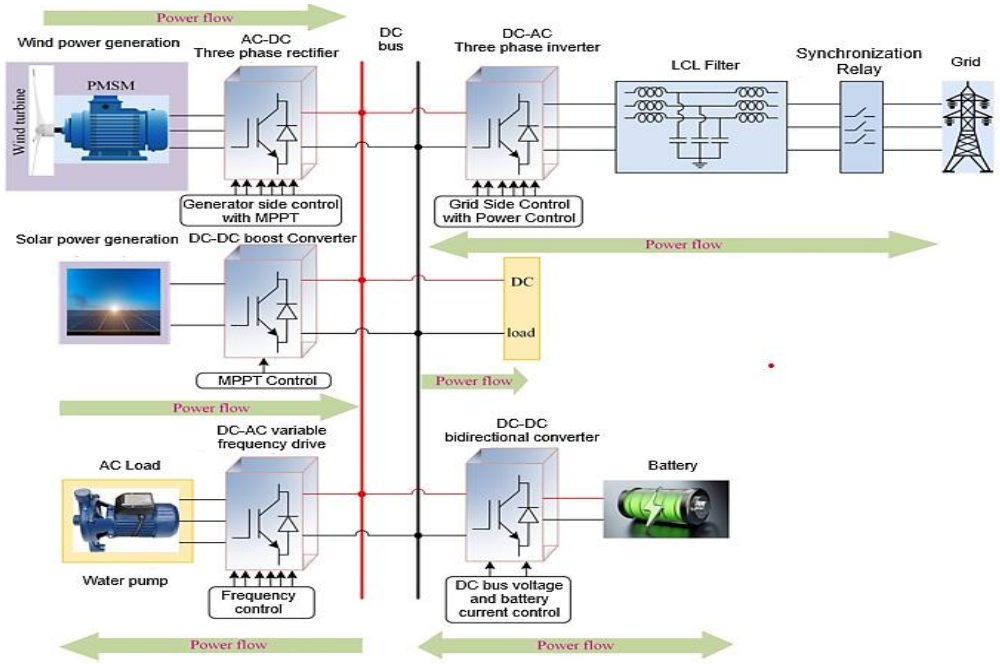

Figure 1. Schematic diagram of the DC/AC microgrid system simplified

FOREX Publication
Open Access | Rapid and quality publishing
International Journal of Electrical and Electronics Research (IJEER)
Review Article | Volume 13, Issue 4 | Pages 943-953 | e-ISSN: 2347-470X

3. PHOTOVOLTAIC MODELING

The analogous PV panel circuit employing an individual diode model is shown in *figure 2*.

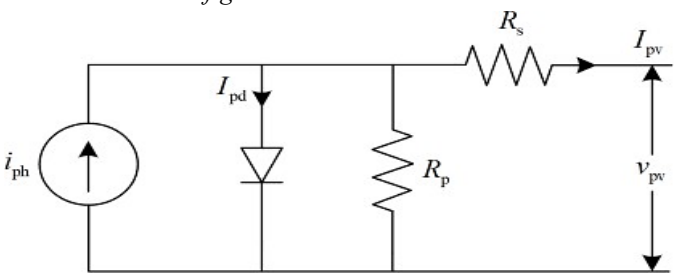

Figure 2. The equivalent circuit representation of a single diode photovoltaic model

$$I_{pv,cell} = I_{ph} - I_{0,pd}\left(e^{\frac{q(V_{pv,cell}+I_{pv,cell}R_{s,pv})}{akT}} - 1\right) - \frac{V_{pv,cell} + I_{pv,cell}R_{s,pv}}{R_{p,pv}} \quad (1)$$

By put on Kirchhoff's Voltage Law (KVL) to *figure 1*, the current of a single cell, denoted as $I_{pv,cell}$ is calculated as follows: where I_{ph} is the photovoltaic current, $I_{0,pd}$ is the current that passes through the parallel diode, along with $R_{p,pv}$ and $R_{s,pv}$, represents the parallel and series resistances of the PV panel, respectively; The output current of a single PV cell is represented by $V_{pv,cell}$, and the output voltage by $V_{pv,cell}$, respectively; The Boltzmann constant is represented by k, the electron charge by q, the ideality factor (curve fitting parameter) by a, and the temperature by T. here maximum solar power is tracked by using circle search algorithm.

4. CIRCLE SEARCH ALGORITHM

Enthused by the geometric structures of circles, the CSA is a new metaheuristic optimization technique that was first presented by Qais et al. [17]. The distance between each point on a circle and its center remains constant, making it a fundamental closed curve. The line segment connecting any two locations on the curve which passes across the center (x_c) is the circle's diameter, while the circle's circumference shows the total length of the encircling curve.

In the circle and distance between any points and its center (x_c) is known as the radius (R). Additionally, With the radius R, the tangent line segment is clearly a straight line which forms a right angle.

According to the Pythagorean theorem, the function of tangent of the right triangle is equal to the combination of the diameter of the circle to the segment of the inclined tangent line. In this instance, the angle of the tangent segment indicates the separation among both points, x_t and x_p. The following equation represents the orthogonal function:

$$Tan(\theta) = \frac{x_t - x_c}{x_p - x_t} \quad (2)$$

Then $$x_t = x_c + (x_p - x_t) * Tan(\theta) \quad (3)$$

To increase the search area for the best answer, the CSA investigates inside circles that are positioned at random. utilizing the circle's center as a point of reference, the angle (θ) that exists between tangent lines point of direct alignment and the circle's perimeter decreases slowly as it gets closer to the circle's center; the angle that occurs when a tangent line joins the point is spontaneously reset because the circle may get stuck in a regional minimum or maximum solution. To increase the search area for the best answer, the CSA investigates inside circles that are positioned at random.

Using the center of the circle as a reference, the angle (θ) in between the tangent lines' points of encounter and also the circle's perimeter progressively decreases as it gets closer to the center.

Randomly determined is the angle where the tangent line touches the point. Since the circle can get stuck in a local minimum or maximum solution.

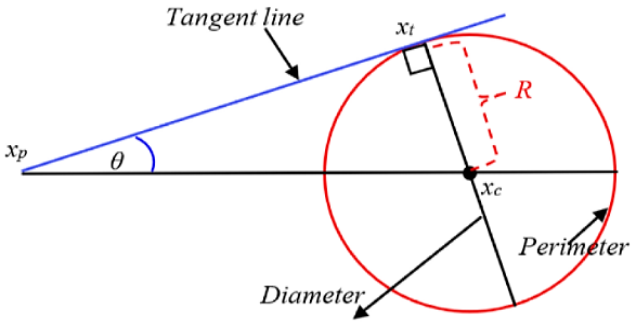

Figure 3. Terminologies of the geometric circle

The tangent point x_t acts as the CSA's search agent, and the algorithm considers the center point x_c to be the ideal location. Furthermore, by moving the tangent point x_t in the direction of the center point x_c, the CSA modifies its search. The tangent point is randomly modified by altering the angle θ in order to keep the algorithm from being trapped in local extrema.

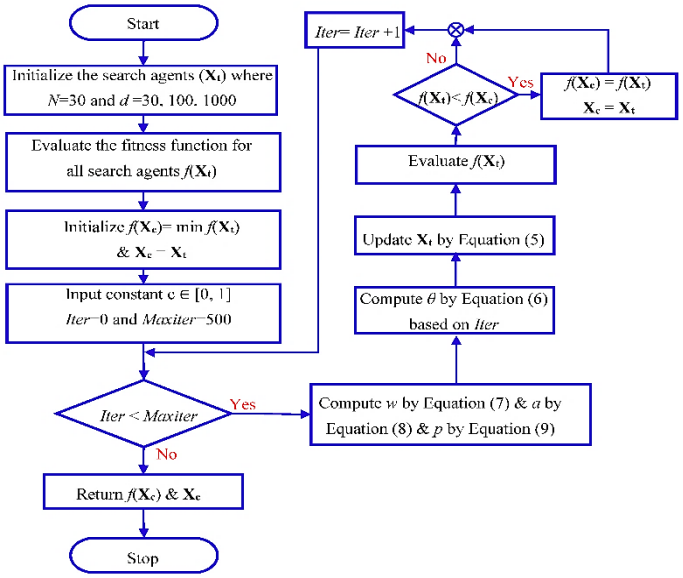

Figure 4. Flowchart of the Circle Search Algorithm

FOREX Publication
Open Access | Rapid and quality publishing
International Journal of Electrical and Electronics Research (IJEER)
Review Article | Volume 13, Issue 4 | Pages 943-953 | e-ISSN: 2347-470X

The PV modules can reliably run at their Maximum Power Point (MPP) under a range of operating situations thanks to the CSA-based maximum power tracking technique, which connects the PV power source with the DC link to extract maximum power than conventional control technique [18].

Phase 1: Initialization: This stage is crucial to the CSA since it guarantees that the search agent's dimensions are all uniformly randomized. The search agents of the CSA are then initialized within the bounds specified by the upper bound (ub) and lower bound (lb) limits of the search space, as shown by *equation (4)*.

$$x_t = up + r * (ub - lb) \quad (4)$$

Here, *r* is a random vector range from 0 to 1.

Phase 2: Changing the Search Agent's Position: Equation illustrates how the search agent's position x_t is modified in this phase by using the most recent best-estimated position x_c.

$$x_t = x_c + (x_c - x_t) * Tan(\theta) \quad (5)$$

In this case, the angle θ, which is essential to investigating and taking advantage of the CSA, can be calculated as follows:

$$\theta = \begin{cases} w * rand & if\ iter > C \\ w * P & otherwise \end{cases} \quad (6)$$

$$W = a * rand - a \quad (7)$$

$$a = \Pi - \Pi * \left(\frac{iter}{maxiter}\right)^2 \quad (8)$$

$$P = 1 - 0.9\sqrt{\frac{iter}{maxiter}} \quad (9)$$

5. GRID SIDE CONVERTER CONTROLLER

A hybrid AC/DC microgrid that combines solar photovoltaic panels, wind-powered permanent magnet synchronous generators, and a battery energy storage system via a shared DC-link is suggested as a solution to these issues [8],[9]. This setup improves system efficiency overall and lowers energy conversion losses. In order to mitigate the voltage sags, swells, and current harmonics, the design employs a Distributed Power Flow Controller (DPFC) to regulate active and reactive power. Because of its special design, it can operate independently and flexibly without heavy DC linkages, which increases power.

A battery energy storage system improves the microgrid's performance by stabilizing DC-link voltage during transient events, sustaining peak load circumstances, and supplying backup power during outages [10]. By transforming linked DC voltage into synchronized 3-Φ AC voltage for power exchange with the grid, the grid-side converter is essential to connecting the hybrid microgrid [11] to the utility grid. By controlling voltage and current, a double-loop control technique guarantees smooth operation even in the face of fluctuating load and generation circumstances.

With an efficient energy management strategy that ensures appropriate distribution of AC and DC loads based on available renewable power and load demands, the proposed microgrid provides seamless operation under both grid-connected and islanded scenarios. Both linear and nonlinear loads are supported by the hybrid structure, and by stabilizing voltage profiles and lowering overall harmonic distortion, the DPFC greatly enhances power quality.

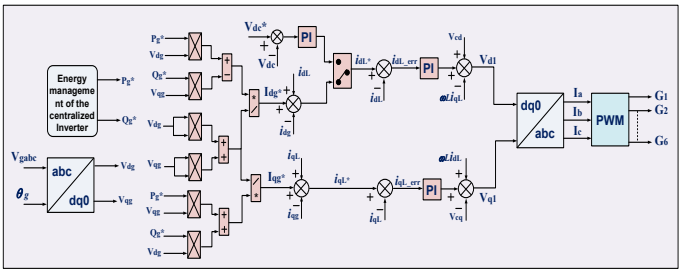

Figure 5. The control diagram illustrating the centralized inverter's connection to the utility grid

The renewable energy source's actual control is as follows:

$$P_{gen} = P_{wind} + P_{solar} + P_{battery} \quad (10)$$

Where $P_{\text{wind}}, P_{battery}, P_{\text{solar}}$ signify power produced by solar and wind, power deposited in battery. The local load's electricity consumption P_{local} given by:

$$P_{local} = P_{ac(pump\ load)} + P_{dc(dc\ load)} \quad (11)$$

Where $P_{dc(dc\ load)}$ and $P_{ac(pump\ load)}$ signify DC load and AC load respectively.

The centralised inverters refer to active power injection is:

$$P_g^* = P_{gen} - P_{local} \quad (12)$$

Where P_g^* denotes position active power.

The references for the *d-q* axis grid current are:

$$i_{dg}^* = \frac{v_{dg}P_g^* - v_{qg}Q_g^*}{v_{dg}^2 + v_{qg}^2} \quad (13)$$

$$i_{qg}^* = \frac{v_{qg}P_g^* - v_{dg}Q_g^*}{v_{dg}^2 + v_{qg}^2} \quad (14)$$

On the *d-q* axis, the variables represent the standard grid current & reactive & active power, respectively. The variables v_{dg} and v_{qg}, on the other hand, indicate the grid voltage on the same *d-q* axis.

To achieve the most efficient transfer of real power to the grid, it is essential to maximize the inductor currents along the reference *d-q* axis. Based on the real inductor currents, instantaneous *d-q* axis references, and actual grid currents, the following formula calculates the inductor currents through the *d-q* axis reference:

FOREX Publication
Open Access | Rapid and quality publishing
International Journal of Electrical and Electronics Research (IJEER)
Review Article | Volume 13, Issue 4 | Pages 943-953 | e-ISSN: 2347-470X

$$i_{dL}^{*} = i_{dg}^{*} + i_{cd} = i_{dg}^{*} + \left(i_{dL} - i_{dg}\right) \quad (15)$$

$$i_{qL}^{*} = i_{qg}^{*} + i_{cd} = i_{qg}^{*} + \left(i_{qL} - i_{qg}\right) \quad (16)$$

Where i_{dL}^{*}, i_{qL}^{*} denote the reference inductor current on the *d-q* axis, i_{dg}^{*}, i_{qg}^{*} the grid current on the *d-q* axis, i_{dL}, i_{qL} the filter inductor current on the *d-q* axis, and i_{cd}, i_{cd} the filter capacitor current on the *d-q* axis may be found. The reference voltages for grid-side control are generated by the inward controller of loop current, which manages errors caused by current from inductor current. To keep the centralized inverter running reliably and steadily, they are used as:

$$v_{dL}^{*} = k_{p,gc}\left(i_{dL}^{*} - \dot{i}_{dL}\right) + k_{i,gc}\int \left(i_{dL}^{*} - i_{dL}\right)dt - \omega L_s i_{qL} + v_{cd} \quad (17)$$

$$v_{qL}^{*} = k_{p,gc}\left(i_{qL}^{*} - \dot{i}_{qL}\right) + k_{i,gc}\int \left(i_{qL}^{*} - i_{qL}\right)dt - \omega L_s i_{dL} + v_{cq} \quad (18)$$

Here, v_{dL}^{*}, and v_{qL}^{*} stand for *d-q* axis inductor reference voltages, $k_{p,gc}$ for the grid current proportional gain controller, and $k_{i,gc}$ for the essential gain of the same controller.

6. DPFC SYSTEM MODELING AND ANALYSIS

An innovative tool used in electrical power systems to improve power flow regulation, transmission reliability, and system flexibility is the Distributed Power Flow Controller (DPFC). It is a development of the Unified Power Flow Controller (UPFC), but by dividing up its functional components, it provides significant structural, financial, and reliability benefits.

In addition to adding a third harmonic current to the system, the shunt converter keeps the bus voltage constant. By injecting voltage in series with the line, the series converters regulate the power flow and are connected to the line *via* single-phase transformers. Instead of using a direct DC link, the third harmonic current is used to transfer energy between series and shunt converters, which improves dependability and streamlines design.

DPFC is able to achieve the intended design configuration through the use of shunt and series inverters. The connections on the CSC are arranged in a left shunt and right series configuration. We present a detailed analysis of the DPFC results in this chapter. The characteristics of the DPFC make it ideal for nonlinear and voltage-sensitive loads.

(i) For non-linear loads, the source current harmonics are decreased and the utility current quality is enhanced.

(ii) DPFC satisfies the load's VAR requirement. It assists in maintaining the source's voltage and current in phase with one another.

(iii) It eliminates the requirement for extra instruments for adjusting power factor

(iv) Regardless of source voltage fluctuations, the DPFC maintains the rated load end voltage.

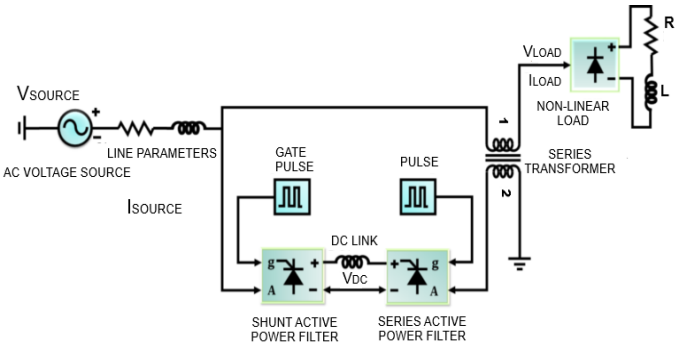

Figure 6. Distributed power flow controllers

The DPFC-PV-WE-ESS system combines renewable energy sources with advanced techniques for monitoring and compensating power quality disturbances. It effectively mitigates voltage issues such as sags, swells, harmonics, and flickers, thereby improving grid reliability and overall operational performance. Leveraging the distributed configuration of the DPFC which includes independently operating series and shunt converters the system enhances control flexibility and responsiveness. The shunt converter plays a key role by providing reactive power compensation and suppressing load current harmonics through the dynamic injection of compensating currents. This functionality ensures seamless integration of renewable sources such as photovoltaic panels for solar energy capture and wind turbines for converting wind energy into electricity.

7. RESULTS AND DISCUSSION

To assess the efficacy of this proposed control technique, simulation tests are performed on a DC/AC hybrid microgrid, considering various wind speeds, irradiation levels, and fluctuating load situations. The system comprises an 8.4KW wind turbine, 4.5KW photovoltaic generating, a 2.2KW lithium-ion battery storage system, a 7.4KW DC load, and a 2.2KW Permanent Magnet Synchronous Motor based water pump. The MATLAB/Simulink program is employed for the simulation analysis, which contrasts the proposed controller with conventional controllers [18] across several situations, including; (1) variations in wind speed & sun radiation. (2) Discrepancy in the Load.

A. The system's performance under varying wind speeds and irradiation conditions.

FOREX Publication
Open Access | Rapid and quality publishing
International Journal of Electrical and Electronics Research (IJEER)
Review Article | Volume 13, Issue 4 | Pages 943-953 | e-ISSN: 2347-470X

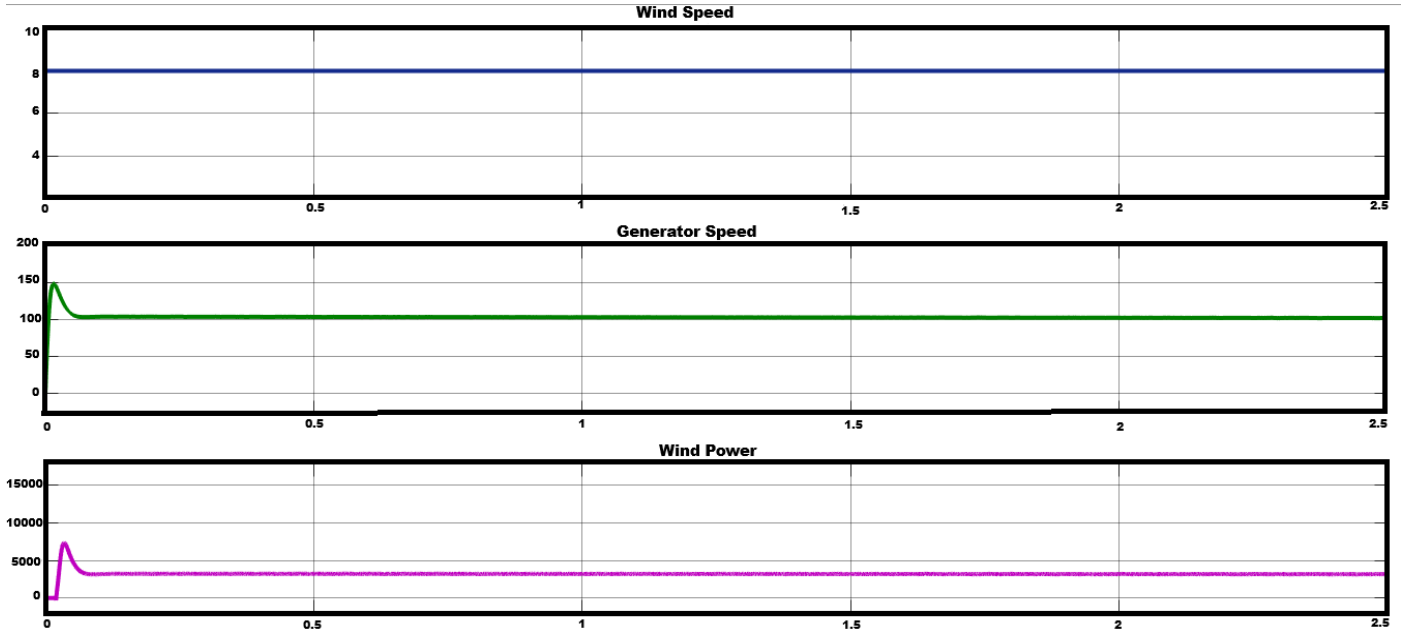

(a) Wind Power Generation

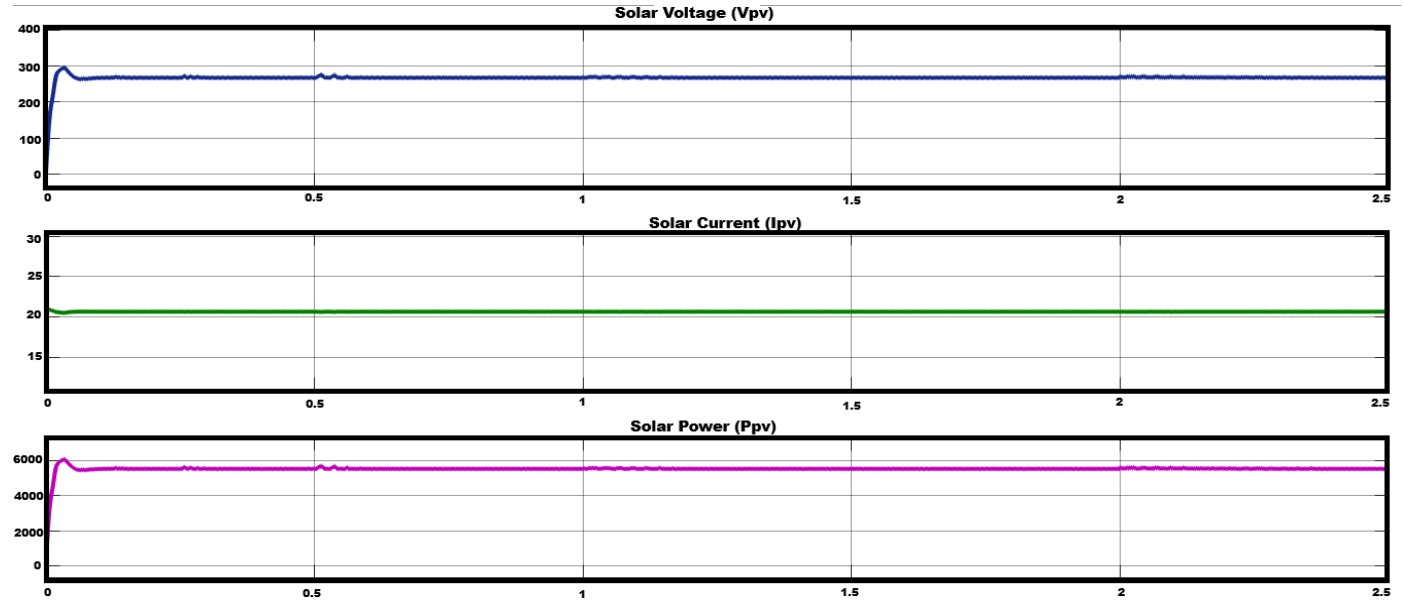

(b) Solar Power Generation

Figure 7. Dynamic system performance at the power generation side under changing wind and radiation conditions. *(a)* wind power generation, *(b)* solar power generation

The *figure 7(a)* shows the dynamic response of the wind energy conversion system (WECS) under a varying wind speed profile. At an average speed of 8 m/s, the PMSG-based turbine generates approximately 3.5 kW at a rotor speed of 100 rad/s. The MPPT algorithm in the machine-side converter continuously adjusts the operating point to track the maximum aerodynamic efficiency. The waveform clearly illustrates how the generator speed and power output rise or fall in accordance with instantaneous wind speed variations, confirming the responsiveness of the tip-speed ratio–based tracking scheme. The smooth power transition indicates proper DC-link stabilization through the bidirectional converter and an effective MSC control loop.

Whereas *figure 7(b)* depicts the voltage, current, and power characteristics of the PV array under fluctuating solar irradiance. Under 1000 W/m², the CSA-based MPPT extracts 5.6 kW, which is significantly higher than conventional controllers. The PV voltage stabilizes around 220 V, and the current reaches 20 A, confirming that the circle search MPPT successfully converges to the true maximum power operating point, even during rapid irradiance changes. The smooth power curve reflects the mitigation of oscillations typically seen in perturbation-based methods, demonstrating higher tracking precision and stability of the proposed algorithm.

FOREX Publication
Open Access | Rapid and quality publishing
International Journal of Electrical and Electronics Research (IJEER)
Review Article | Volume 13, Issue 4 | Pages 943-953 | e-ISSN: 2347-470X

B. Performance of the system for mitigation of power quality issues using DPFC

At first, 15.1KW of power is generated by a wind turbine, solar panel, and battery, 7.4KW is used by the DC load, and 5.4KW is pumped into the grid. Then the performance of the total system is roughly 95.5%. Additionally, the system responds smoothly when the load condition changes due to the suggested controller, which also uses DPFC to eliminate power quality problems.

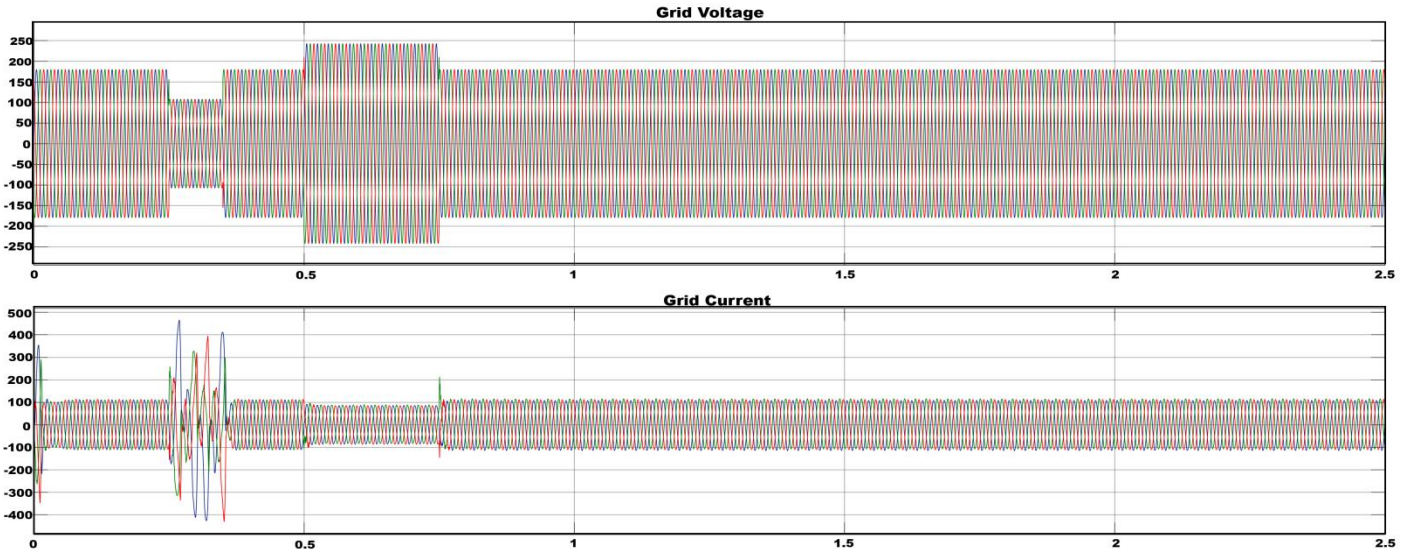

Figure 8. Grid current and voltage before compensation

Figure 8 shows the uncompensated grid voltage and current waveforms where sag and swell disturbances are visible at different time instants. A voltage sag is observed from 0 to 1.3ms, representing a temporary reduction in the system voltage due to sudden load increase or source disturbance. A voltage swell occurs between 0.5 and 0.7ms, caused by a decrease in load or transient energy injection.

These deviations directly propagate into the grid current, showing distortion and imbalance. The figure highlights the severity of unmitigated power quality issues in renewable-integrated microgrids and establishes the necessity for DPFC compensation.

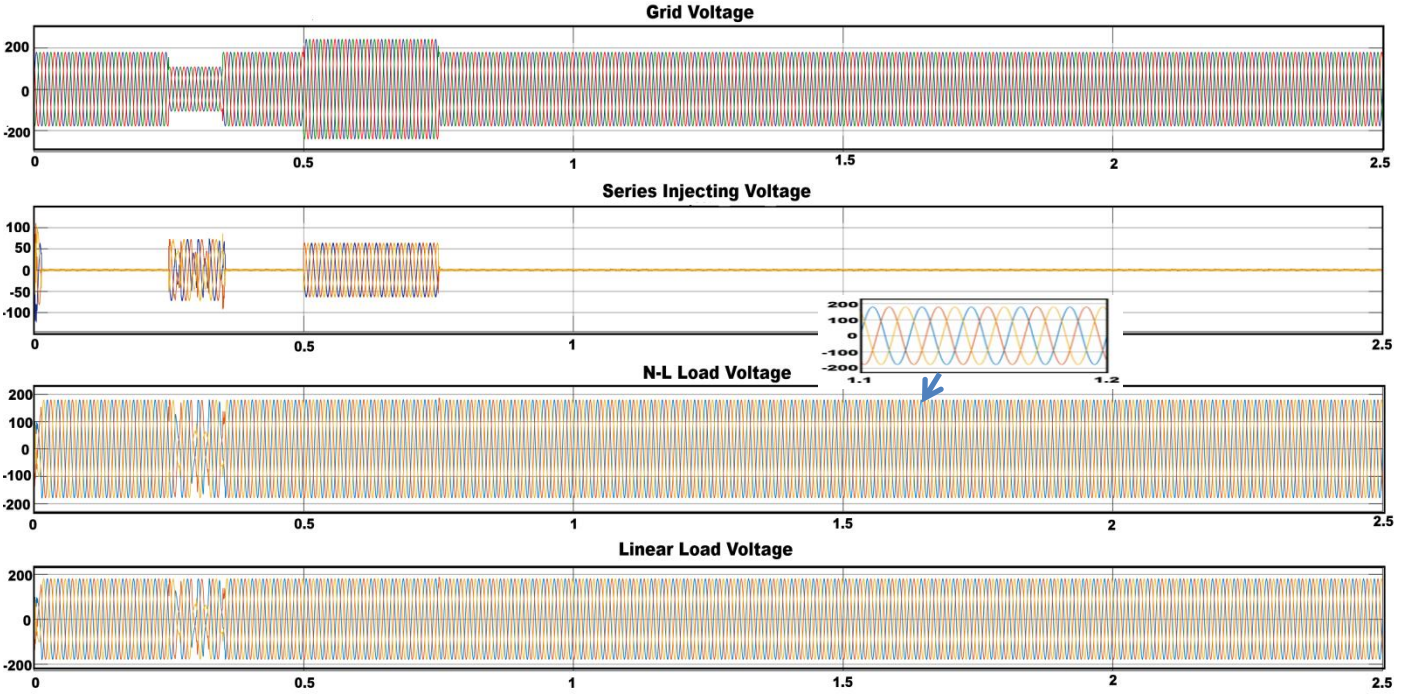

Figure 9. Grid voltage, Series injected voltage, N_L load, Linear Load current

FOREX Publication
Open Access | Rapid and quality publishing
International Journal of Electrical and Electronics Research (IJEER)
Review Article | Volume 13, Issue 4 | Pages 943-953 | e-ISSN: 2347-470X

This figure illustrates the action of the DPFC series converter, which injects a compensating voltage into the line to counteract the observed sag and swell. The injected voltage waveform is inverted and shifted appropriately to restore the grid voltage to nominal levels. During sag periods, the series converter injects positive voltage to raise the line voltage. During swell periods, it injects negative voltage to suppress the excess voltage. The stabilized load voltage waveform confirms the accurate synchronization of the series converter and demonstrates effective mitigation of both linear and nonlinear load distortions.

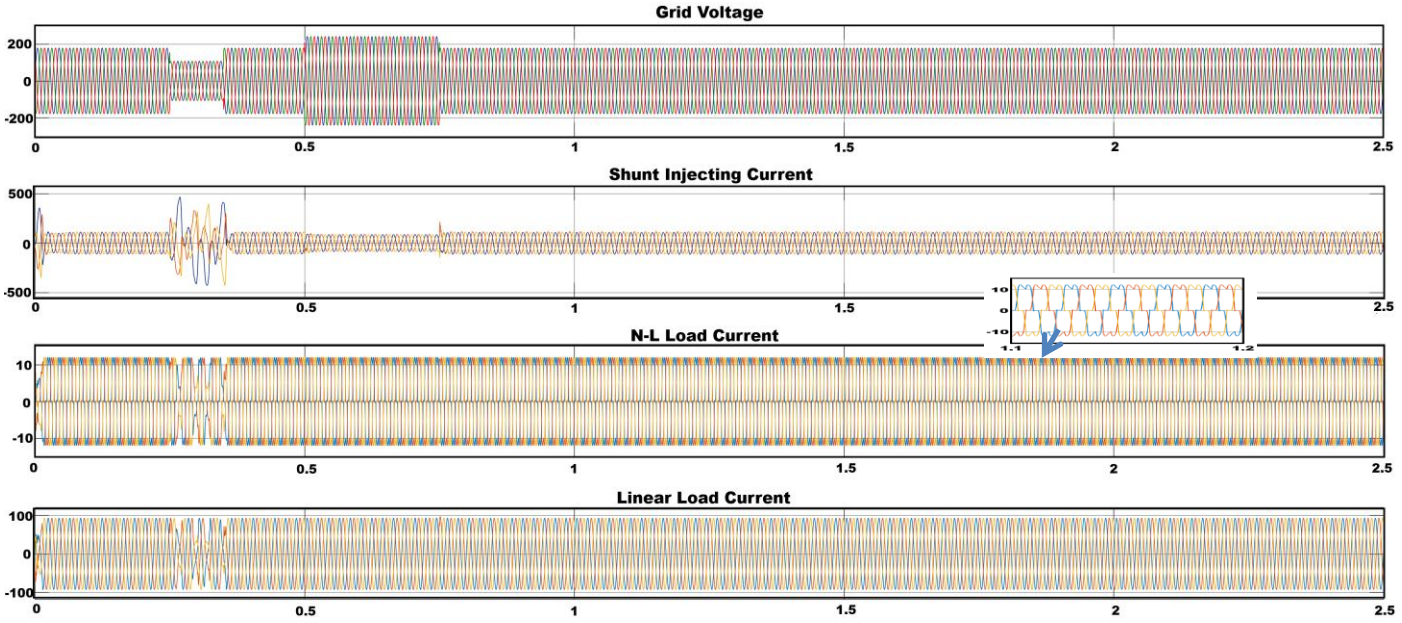

Figure 10. Grid voltage, Shunt injected current, N_L load, Linear Load current

Figure 10 presents the action of the DPFC shunt converter, which injects compensating current into the grid to correct current-related disturbances. A sag between 0.25–0.35 s and swell between 0.45–0.75s are clearly observed. The shunt converter injects a harmonic-suppressing and reactive power compensating current that forces the grid current into a clean sinusoidal waveform. The improvement is evident as the compensated current closely aligns in phase with the restored grid voltage, indicating proper reactive power support and harmonic cancellation.

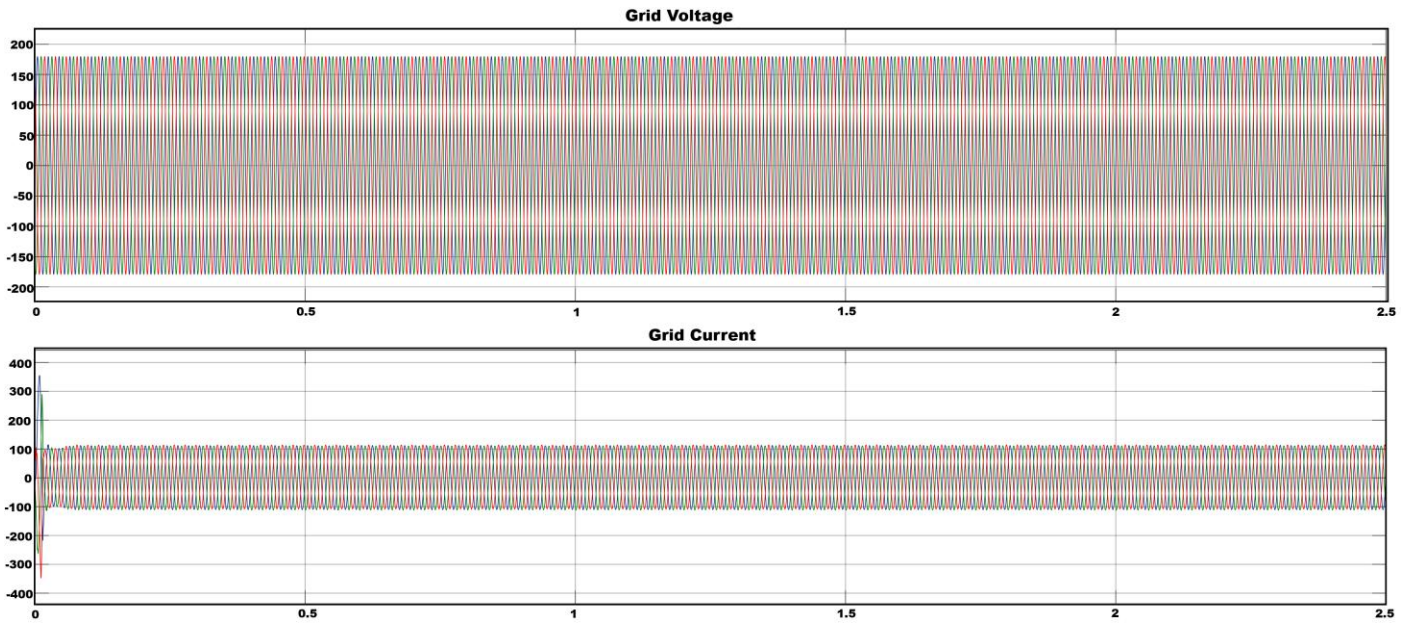

Figure 11. Grid voltage and current after compensation

FOREX Publication
Open Access | Rapid and quality publishing
International Journal of Electrical and Electronics Research (IJEER)
Review Article | Volume 13, Issue 4 | Pages 943-953 | e-ISSN: 2347-470X

This figure demonstrates the final grid voltage and current waveform after both series and shunt DPFC compensation. The voltage waveform is completely restored to its nominal magnitude without any sag or swell. The grid current becomes purely sinusoidal with proper phase alignment, confirming elimination of harmonics and reactive components. This figure validates that DPFC achieves full PQ restoration under dynamic load and supply disturbances, enabling stable grid operation.

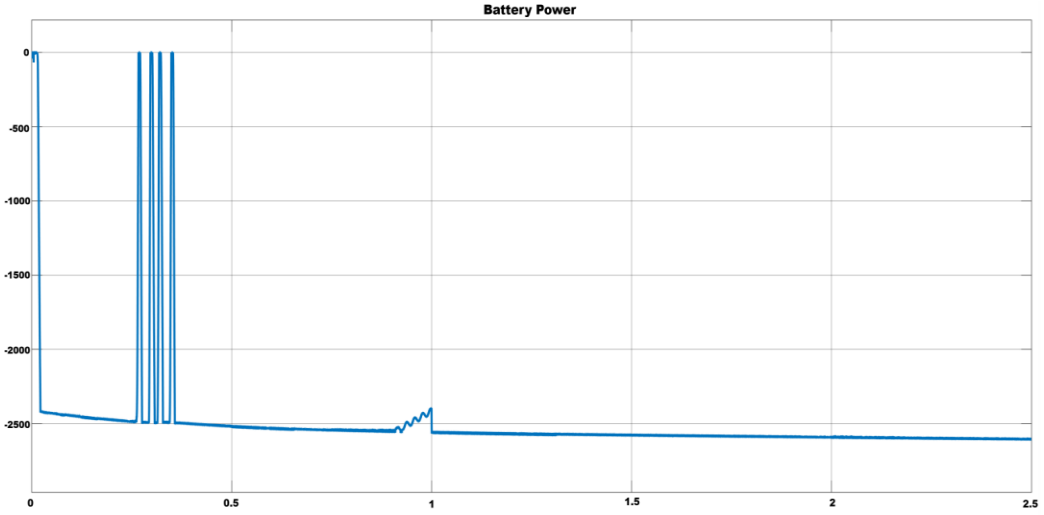

Figure 12. Battery power of the EV

Figure 12 displays the power flow pattern of the EV battery connected through the DC link of the DPFC. The Negative values indicate charging, meaning the battery absorbs power from the microgrid. The Positive values indicate discharging, meaning the battery supplies power back to the system. The transitions between charging and discharging highlight the successful coordination between renewable power availability, load demand, and storage requirements. This confirms the effectiveness of the energy management strategy in maintaining DC-link stability.

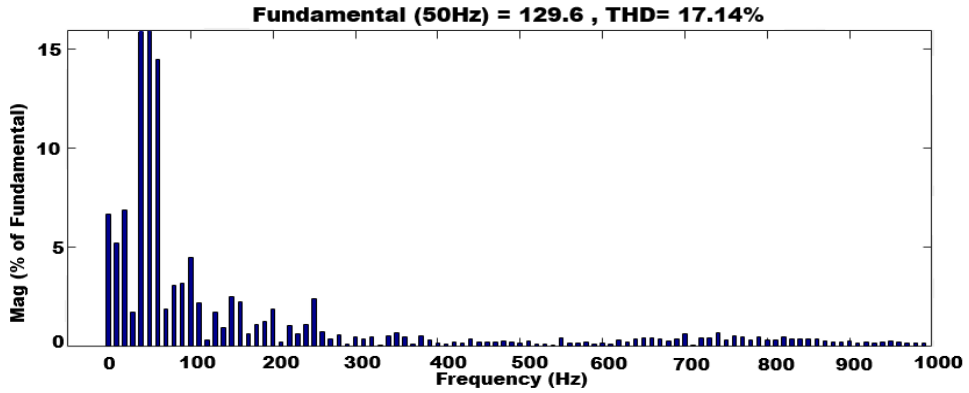

(a) Without Compensation of Harmonic Current

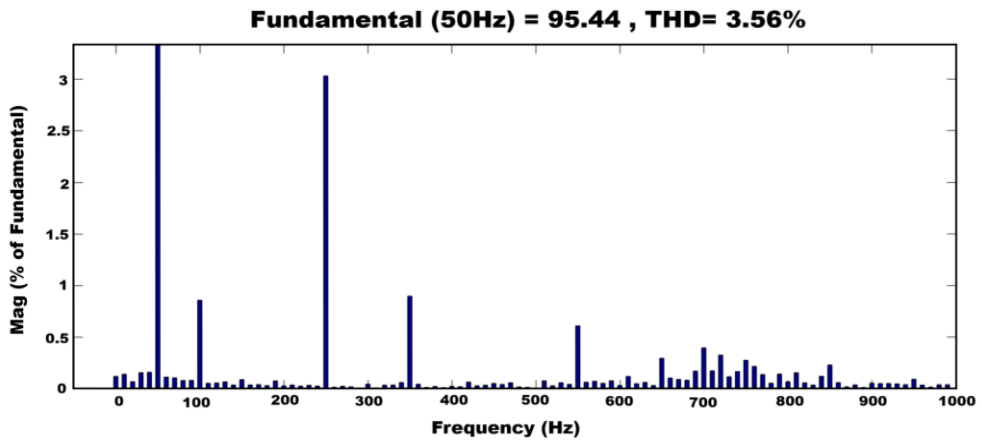

(b) With Compensation of Harmonic Current

FOREX Publication
Open Access | Rapid and quality publishing
International Journal of Electrical and Electronics Research (IJEER)
Review Article | Volume 13, Issue 4 | Pages 943-953 | e-ISSN: 2347-470X

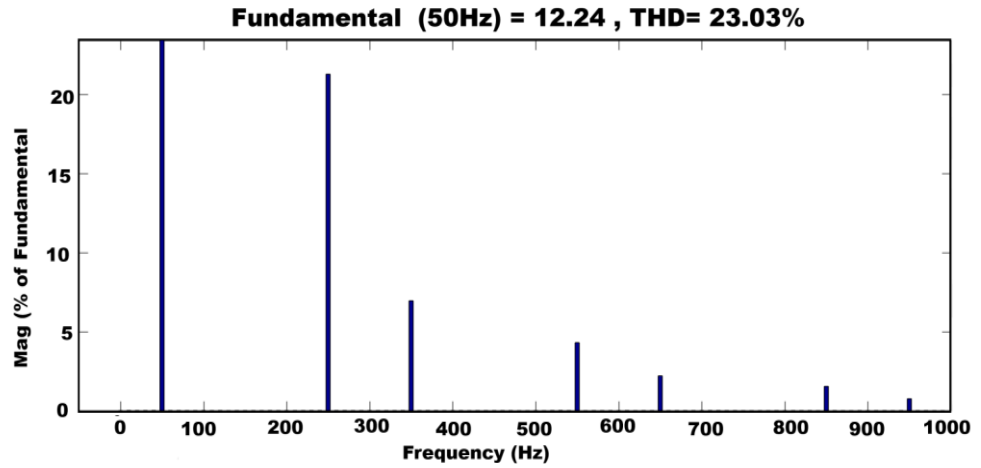

(c) Without Compensation of Load Harmonic

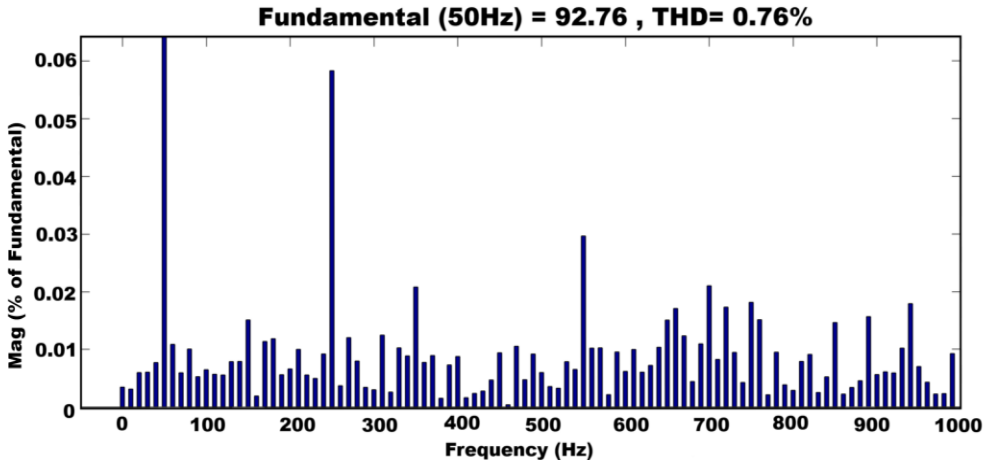

(d) with Compensation of Load Harmonic

Figure 13. Harmonic analysis of without and with DPFC

This multi-part figure illustrates the harmonic spectrum of the grid current and load current before and after compensation:*(a)* Grid Harmonics Without Compensation The THD is around 17.14%, showing significant distortion due to nonlinear loads.*(b)* Grid Harmonics With Compensation After applying shunt compensation, THD reduces to 3.56%, within IEEE-519 limits.*(c)* Load Harmonics Without Compensation The nonlinear load draws highly distorted current with a THD of 23.03%.*(d)* Load Harmonics With Compensation Series–shunt DPFC compensation reduces THD to 0.76%, confirming excellent harmonic filtering capability.

TABLE 1. Performance assessment of the suggested using the traditional MPPT method [18]

Solar Irradiation	Proposed	Conventional
Solar Power	5.6KW at 1000W/m^2	4350W at 1000W/m^2
Solar Current	20A	18.4A
Solar Voltage	220V	160V

TABLE 2. THD Comparison Using DPFC with and Without Compensation

Total harmonics distortion	without compensation	with compensation
Harmonic Current	17.14%	3.56%
Load Harmonics	23.03%	0.76%

8. CONCLUSION

This work presented a coordinated control strategy for a hybrid DC/AC microgrid integrating solar PV, wind energy, and a battery energy storage system, enhanced with a Distributed Power Flow Controller (DPFC) for power quality improvement. The major technical contributions include the development of a Circle Search Algorithm (CSA) based MPPT for PV systems, a tip-speed ratio–based controller for PMSG wind turbines, and a dual-loop inverter control scheme that ensures optimal power flow between renewable sources, storage, and the utility grid. The proposed system demonstrates significant system-level benefits by maintaining a stable DC-link voltage, ensuring reliable power delivery to AC and DC loads, and enabling seamless grid-connected and islanded operation. The coordinated control enhances renewable energy utilization,

FOREX Publication
Open Access | Rapid and quality publishing
International Journal of Electrical and Electronics Research (IJEER)
Review Article | Volume 13, Issue 4 | Pages 943-953|e-ISSN: 2347-470X

reduces dependency on the utility grid, and ensures smooth load-sharing among PV, wind, and battery units.

Quantitative results confirm notable improvements in power quality. Harmonic distortion is reduced from 17.14% to 3.56% in grid current and from 23.03% to 0.76% in load current, meeting IEEE-519 standards. Likewise, the CSA-based MPPT increases PV power extraction to 5.6 kW, outperforming conventional techniques. Voltage sag and swell disturbances are effectively compensated by the DPFC, restoring the grid voltage to nominal levels and improving current sinusoidal. The validated simulation results under varying wind speed, fluctuating irradiance, and load disturbances demonstrate the practical applicability of the proposed system for real-world renewable-integrated distribution networks. Overall, the proposed coordinated control and DPFC-driven compensation framework significantly enhances the stability, reliability, and power quality of hybrid microgrid systems.

Funding: This research received no external funding.

Conflicts of Interest: The authors declare no conflict of interest.

REFERENCES

[1] A. I. M. Ali and H. R. A. Mohamed, ‘‘Improved P&O MPPT algorithm with efficient open-circuit voltage estimation for two-stage grid-integrated PV system under realistic solar radiation,’’ Int. J. Electr. Power Energy Syst., vol. 137, May 2022, Art. no. 107805.

[2] K. Saidi, M. Maamoun and M. Bounekhla, "Simulation and implementation of incremental conductance MPPT algorithm with indirect control method using buck converter," 2017 6th International Conference on Systems and Control (ICSC), Batna, Algeria, 2017, pp. 199-204.

[3] Yassine El Alami, Elmostafa Chetouani, Hamza Mokhliss, Fatima Ouerradi, Mohssin Aoutoul, Said Bounouar, Rachid Bendaoud, Ahmed Faize, Redouane Rmaily, Optimizing solar energy efficiency with an improved hill-climbing maximum power point tracking control approach: hardware implementation, *Clean Energy*, Volume 8, Issue 5, October 2024, Pages 167–176.

[4] Y. Li, Z. Xu and K. P. Wong, "Advanced Control Strategies of PMSG-Based Wind Turbines for System Inertia Support," in IEEE Transactions on Power Systems, vol. 32, no. 4, pp. 3027-3037, July 2017, doi: 10.1109/TPWRS.2016.2616171.

[5] de Oliveira, F. M., Brandt, M. H. M., Salvadori, F., Izquierdo, J. E. E., Cavallari, M. R., & Ando Junior, O. H. (2024). Development of an MPPT-based genetic algorithm for photovoltaic systems versus classical MPPT techniques in scenarios with partial shading. *Inventions*, *9*(3), 64.

[6] Sajid, I., Sarwar, A., Tariq, M., Ahmad, S., Bakhsh, F. I., Mohamed, A. S. N., & Islam, M. R. (2024). An MPPT method using phasor particle swarm optimization for PV-based generation system under varying irradiance conditions. *IET Renewable Power Generation*, *18*(16), 4197-4209.

[7] M. Huang, Z. Zhang, W. Wu and Z. Yao, "An Improved Three-Level Cascaded Control for LCL-Filtered Grid-Connected Inverter in Complex Grid Impedance Condition," in IEEE Access, vol. 10, pp. 65485-65495, 2022.

[8] Li, X., Dong, C., Jiang, W., & Wu, X. (2021). An improved coordination control for a novel hybrid AC/DC microgrid architecture with combined energy storage system. *Applied Energy*, *292*, 116824.

[9] Antalem, D. T., Muneer, V., & Bhattacharya, A. (2022). Decentralized control of islanding/grid-connected hybrid DC/AC microgrid using interlinking converters. *Science and Technology for Energy Transition*, *77*, 22.

[10] T. A. Fagundes et al., "Battery Energy Storage Systems in Microgrids: A Review of SoC Balancing and Perspectives," in IEEE Open Journal of the Industrial Electronics Society, vol. 5, pp. 961-992, 2024, doi: 10.1109/OJIES.2024.3455239.

[11] Armghan, H., Xu, Y., Ali, N., & Farooq, U. (2024). Coordination control in hybrid energy storage based microgrids providing ancillary services: A three-layer control approach. *Journal of Energy Storage*, *93*, 112221.

[12] Abdelwanis, M. I., & Elmezain, M. I. (2024). A comprehensive review of hybrid AC/DC networks: insights into system planning, energy management, control, and protection. *Neural Computing and Applications*, *36*(29), 17961-17977.

[13] Goud, B. S., Reddy, C. R., Bajaj, M., Elattar, E. E., & Kamel, S. (2021). Power quality improvement using distributed power flow controller with BWO-based FOPID controller. *Sustainability*, *13*(20), 11194.

[14] T. E. Rao, E. Sundaram, S. Chenniappan, D. Almakhles, U. Subramaniam and M. S. Bhaskar, "Performance Improvement of Grid Interfaced Hybrid System Using Distributed Power Flow Controller Optimization Techniques," in IEEE Access, vol. 10, pp. 12742-12752, 2022, doi: 10.1109/ACCESS.2022.3146412.

[15] M. J. M. A. Rasul, H. V. Khang and M. Kolhe, "Harmonic mitigation of a grid-connected photovoltaic system using shunt active filter," 2017 20th International Conference on Electrical Machines and Systems (ICEMS), Sydney, NSW, Australia, 2017, pp. 1-5.

[16] S. B. Anawade and A. A. Kale, "Series Active Power Filter (SAPF) For Power Quality Improvement," 2022 Interdisciplinary Research in Technology and Management (IRTM), Kolkata, India, 2022, pp. 1-9.

[17] M. H. Qais, H. M. Hasanien, R. A. Turky, S. Alghuwainem, M. Tostado-Véliz, and F. Jurado, ‘‘Circle search algorithm: A geometry-based metaheuristic optimization algorithm,’’ Mathematics, vol. 10, no. 10, p. 1626, May 2022.

[18] P. K. Kesavan, U. Subramaniam, D. J. Almakhles and S. Selvam, "Modelling and Coordinated Control of Grid Connected Photovoltaic, Wind Turbine Driven PMSG, and Energy Storage Device for a Hybrid DC/AC Microgrid," in Protection and Control of Modern Power Systems, vol. 9, no. 1, pp. 154-167, January 2024, doi: 10.23919/PCMP.2023.000272.

[19] Agarwal, N. Kr., Saxena, A., Prakash, A., Singh, A., Srivastava, A., & Baluni, A. (2021). Review on Unified Power Quality Conditioner (UPQC) to Mitigate Power Quality Problems. *2021 2nd Global Conference for Advancement in Technology (GCAT)*, 1–7.

[20] Heenkenda, A., Elsanabary, A., Seyedmahmoudian, M., Mekhilef, S., Stojcevski, A., & Aziz, N. F. A. (2023). Unified Power Quality Conditioners based Different Structural Arrangements: A Comprehensive Review. *IEEE Access*, *11*, 43435–43457.

[21] Alam, Md. S., Al-Ismail, F. S., Salem, A., & Abido, M. A. (2020). High-level penetration of renewable energy sources into grid utility: Challenges and solutions. *IEEE Access, 8,* 190277–190299.

[22] Bajaj, M., & Singh, A. K. (2020). Grid Integrated Renewable DG Systems: A Review of Power Quality Challenges and State-of-the-Art Mitigation Techniques. *International Journal of Energy Research, 44*(1), 26–69. Mlilo, N., Brown, J., & Ahfock, T. (2021). Impact of intermittent renewable energy generation penetration on the power system networks – A review. *Technology and Economics of Smart Grids and Sustainable Energy, 6*(1), 25.

[23] Diab, A. M., Bozhko, S., Guo, F., Rashed, M., Buticchi, G., Xu, Z., Yeoh, S. S., Gerada, C., & Galea, M. (2021). Fast and Simple Tuning Rules of Synchronous Reference Frame Proportional-Integral Current Controller. *IEEE Access*, *9*, 22156–22170.